Electrocatalytic Oxidation of Formic Acid on Pd/Ni Heterostructured Catalyst

Mingjun Ren[1,2], Liangliang Zou[1,2], Ju Chen[1], Ting Yuan[1,2], Qinghong Huang[1], Haifeng Zhang[1], Hui Yang[1*], Songlin Feng[1]

(1. *Shanghai Advanced Research Institute, Chinese Academy of Sciences (CAS), Shanghai* 201210, *China;* 2. *Graduate School of the CAS, Beijing* 100039, *China*)

Abstract:　A Pd/Ni bimetallic nanostructured electrocatalyst was fabricated via a two-step reduction route. Owing to an epitaxial growth of Pd atoms on the surface of Ni nanoparticles, heterostructured Pd/Ni nanocomposites were formed and verified by high resolution transmission electron microscopy combined with energy-dispersion X-ray spectroscopy. X-ray diffraction confirmed that the as-prepared Pd/Ni nanocomposites possessed a single face-centered-cubic (fcc) Pd structure, probably due to a weaker diffraction intensity of metallic Ni and/or overlapping by that of Pd. The intrinsic catalytic activity on the Pd/Ni is higher than that on the Pd. Moreover, the durability of formic acid oxidation on the Pd/Ni was much enhanced over the Pd nanoparticles. The change in electronic structure of the surface coordination unsaturated Pd atoms and the possible dissolution of Ni species from the Pd/Ni heterostructure may account for such an improved durability for formic acid oxidation.

Key words:　formic acid oxidation; electrocatalysis; Pd/Ni heterostructure; durability

CLC Number:　O646　　　　　　　　　　　**Document Code:**　A

1　Introduction

　　Direct formic acid fuel cell (DFAFC) has attracted much attention for portable application due to its high energy density, facile power-system integration, nontoxic, and convenient storage and transport of liquid formic acid[1-3]. For the DFAFCs, Pd-based nanostructured materials have been commonly used as anode catalysts; generally because of their high catalytic activity for formic acid oxidation, but also because of lower cost and greater abundance than Pt[4]. Recent studies have shown that Pd is an efficient catalyst for formic acid oxidation to final product CO_2 through a "direct pathway", which could overcome the $(CO)_{ad}$ poisoning effect and thereby yield a high performance in a DFAFC[4].

However, the very limited durability of Pd-based catalysts for formic acid oxidation has seriously restricted the practical application of the DFAFC. Therefore, synthesis of modified Pd based nanocatalysts with improved durability for formic acid oxidation still remains a big challenge.

　　Several strategies have been utilized for the modification of the Pd to enhance the durability of the catalyst for formic acid oxidation. Generally, the modification of the Pd by a second metal would result in an improved performance due to synergistic effect and to the change in electronic structure in the surface coordination unsaturated atoms (CUS). For example, Wang et al reported a PdCo/C catalyst with the improved activity and durability relative to

their as-prepared Pd/C[5]. Haan and his colleagues prepared a novel PdSb nanostructured catalyst that exhibits enhanced durability over the Pd/C during the electrocatalytic oxidation of formic acid[6]. Theory investigation based on density functional theory by Nørskov et al. also suggests that the modification of Pd by the other transition metals will lead to a variation in d-band center, and thus the electrocatalytic properties would be improved significantly [7-8]. Furthermore, the modification of Pd by Ni would lead to the decrease in d-band center, which will improve the CO-tolerance[8-9].

In this work, aiming at the improved durability for formic acid oxidation, the heterostructured catalyst of Pd decorated on the surface of Ni nanoparticles was prepared. Its electrocatalysis for formic acid oxidation was investigated and compared with that of Pd nanoparticles. The formation of heterostructure and the effect of electronic structure on formic acid oxidation will be discussed in detail.

2　Experimental

The Pd/Ni catalyst was synthesized by a two-step reduction route under the protection of high-purity nitrogen in an iced bath. Firstly, 8 mL of 0.2 mol·L^{-1} Ni(NO$_3$)$_2$, 5 mL of 64 mmol·L^{-1} sodium citrate and 50 mL of ultra-pure water were mixed ultrasonically for 15 min. Then, 10 mL of 1.6 mol·L^{-1} NaBH$_4$ solution was added into the above mixture at a rate of 20 mL·h^{-1} under vigorous stirring, leading to the formation of Ni nanoparticles. In second step, both 20 mL of 40 mmol·L^{-1} Na$_2$PdCl$_4$ solution and 20 mL of 0.16 mol·L^{-1} NaBH$_4$ solution were synchronously added into the solution of Ni nanoparticles at a rate of 20 mL·h^{-1}. The mixture was stirred for another 60 min. Then, the resultant catalyst was filtrated and washed with ultra-pure water for more than three times. For the preparation of Pd nanoparticles, only the second step was performed.

XRD measurements were conducted using a Bruke D8 Advanced XRD diffractometer with Cu K_{α_1} radiation （λ = 0.154 06 nm). The tube voltage was maintained at 40 kV and the tube current at 100 mA. Diffraction patterns were collected at a scanning rate of 2°·min^{-1} and a step size of 0.02°. The morphology of the catalysts was characterized using a JEOL JEM-2100F TEM with an energy-dispersive X-ray spectroscopy (EDS) detector operated at 200 kV. The samples were prepared by ultrasonically suspending catalyst power in ethanol. A drop of suspension was then placed onto a holey copper grid and dried under air. The analysis of the atomic composition of the catalyst was performed with an IRIS advantage inductively coupled plasma atomic emission spectroscopy (ICP-AES).

Electrochemical experiments were carried out using Solartron Electrochemical Interface SI1287 with a standard three-electrode cell. 10 mg of the catalyst, 0.5 mL of 5wt.% Nafion solution, and 2.5 mL of ultrapure water were mixed ultrasonically to form the catalyst ink. Subsequently, 3 μL of such a mixture was transferred onto the surface of glassy carbon (GC, 3 mm in diameter) electrode. The electrolyte used was 0.5 mol·L^{-1} H$_2$SO$_4$ or 0.5 mol·L^{-1} H$_2$SO$_4$+ 0.5 mol·L^{-1} HCOOH solution. High purity nitrogen was introduced for the deaeration of the solutions. To determine the real electrochemical surface area （ECSA) of the catalyst, cyclic voltammograms （CVs) and CO-stripping voltammograms were conducted. For the CO-stripping, CO was pre-adsorbed at an open circuit potential for 30 min by bubbling CO into 0.5 mol·L^{-1} H$_2$SO$_4$ solution, and then CO dissolved in solution was subsequently removed by purging high-purity N$_2$ for 30 min. In all cases, electrochemical measurements were conducted at a temperature of （25 ± 1) ℃.

3　Results and Discussion

Morphologies of the Pd/Ni and Pd nanoparticles were investigated using TEM technology. Fig. 1A indicates that the Pd/Ni is a nanostructured material with an average particle size of ca. 5.1 nm based on the observation of more than 100 isolated particles. In contrast, the mean particle size of pure Pd nanoparticles is ca. 4.8 nm, as estimated from Fig. 1B. From the Fig. 1A and 1B, one can observe a serious aggregation for both the Pd/Ni and Pd

nanoparticles. High-resolution TEM image in Fig. 1C demonstrates that the Pd/Ni nanocomposite is composed of two parts, as lined out with green and red frames. The observed result is fully repeatable. A farther investigation using EDS indicates that the two parts are Pd and Ni, respectively, as shown in Fig. 1D and 1E, clearly demonstrating the formation of the heterostructured Pd/Ni nanocomposites. The conclusion is confirmed by the results with selected area electron diffraction (SAED), as can be seen in Fig. 1D and 1E. The appearance of Ni element in the Pd parts, as well as the appearance of Pd element in the Ni parts, may be due to Kirkendall effect, which results in atoms diffusion in the junctions of the particles. The heterostructure formation may be due to an inherent lattice mismatch between Pd and Ni[10]. Once the reduction reaction of $PdCl_4^{2-}$ ions occurs, the Pd atoms prefer to the epitaxial growing on the surface of the Ni nanoparticles, rather than self-nucleation, owing to a lower Gibbs free energy for the growth than nucleation[11]. Subsequently, because of a large lattice mismatch between Pd and Ni, the Gibbs free energy for the growth on the Pd is lower than that on the Ni, and then the Pd atoms will continue to grow on the surface of the formed Pd. Finally, the atomic ratio of the Pd/Ni is very close to 1:2, as confirmed by ICP-AES techniques.

Fig. 2 shows the XRD patterns of the Pd/Ni and Pd catalysts. For a comparison, the diffraction peaks of both metallic Pd (JCPDF Card No. 87-0641) and Ni (JCPDF Card No. 65-2865) are also given in the Fig. 2, corresponding to the blue dash and red dot lines, respectively. Both prepared samples exhibit a typical characteristic diffraction patterns of the Pd fcc structure[12-13]. No remarkable diffraction peaks, assigned as metallic Ni, were observed, indicating that the Pd/Ni composites also have a single fcc structure. Such a conclusion is not in agreement with TEM results, probably due to a weaker diffraction intensity of the Ni and overlapping by that of Pd. In addition, the diffraction peak located at ca. 30° can be ascribed to the Pd oxides for the Pd nanoparticles[4]. The average particle sizes for the Pd/Ni and Pd nanoparticles, as calculated from the diffraction peak (220) using Scherrer's equation, are 4.4 and 4.1 nm, respectively. The obtained values are slightly smaller than that by TEM. The estimated mean particle size of the Ni nanoparticles before Pd reduction is ca. 3 nm by using Scherrer's equation, indicating that the mean thickness of Pd in the Pd/Ni nanocomposites is ca. 1.4 nm.

Fig. 3 presents the CVs and the CO-stripping profiles of the Pd/Ni and Pd catalysts, and all of the currents were normalized to the $ECSAs_H$ or $ECSAs_{CO}$. As can be seen in Fig. 3A, both catalysts show the
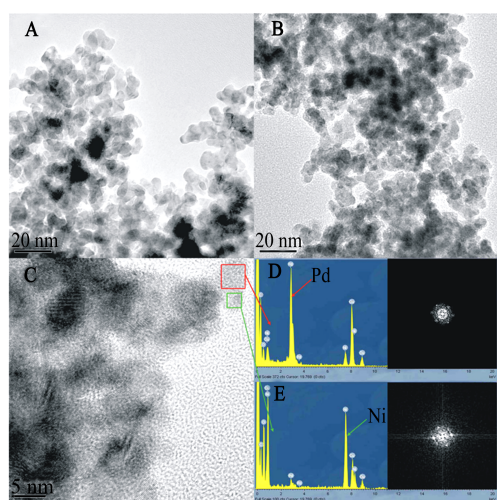

Fig. 1 TEM images of the Pd (A) and Pd/Ni (B) catalysts, HR-TEM image of the Pd/Ni catalyst (C), and EDS with corresponding SEAD results from separated parts of a single Pd/Ni nanoparticle (D and E).
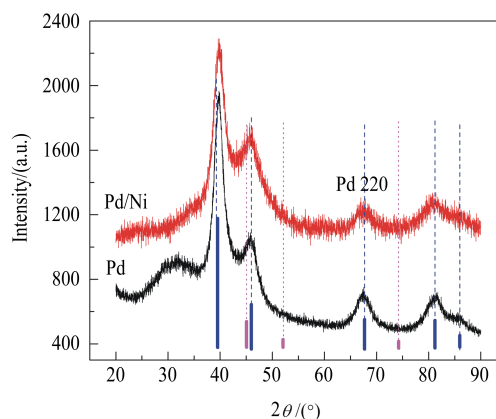

Fig. 2 XRD patterns of the as-prepared Pd/Ni and Pd nanocatalysts. The blue dash and magenta dot lines are the diffraction lines of the metallic Pd and the Ni from JCPDF cards 87-0641 and 65-2865, respectively.

typical hydrogen adsorption/desorption region of the Pd. By calculating hydrogen desorption region area, the specific ECSAs$_H$ can be estimated as 3.50 and 10.08 m^2·g^{-1} for the Pd/Ni and Pd nanoparticles, respectively. Similarly, the specific ECSAs$_{CO}$ calculated from CO oxidation peak in Fig. 3B are 3.82 and 11.17 m^2·g^{-1} for the Pd/Ni and Pd catalysts. Interestingly, the CO oxidation peak on the Pd/Ni shifts negatively relative to that on the Pd nanoparticles, probably revealing that the CO-like species, produced during the formic acid oxidation, can be removed more easily. This can be ascribed to the change in the electronic structure, probably caused by the Ni atoms diffusion into the Pd at the Pd/Ni junctions. Normally, the down-shift of the d-band center implies less electrons in the 4d orbit of the CUS Pd can be back-donated to the 2π* orbit of (CO)$_{ad}$. Thus, the bonds formed between CO and the CUS surface Pd atoms on the Pd/Ni are weaker than that on the Pd. Consequently, the Pd/Ni exhibits an enhanced CO-tolerance[8-9,14].

　　The electrocatalytic activity of formic acid oxidation on both the catalysts was evaluated in 0.5 mol·L^{-1} HCOOH + 0.5 mol·L^{-1} H$_2$SO$_4$ solution, and the current was normalized to the ECSAs$_{CO}$. From Fig. 4A, one can see that the peaks of the oxidation currents on the Pd/Ni are higher than that on the Pd, indicating that the electrocatalytic activity on the Pd/Ni is higher than that on pure Pd nanoparticles.

Furthermore, the durability of the Pd/Ni catalyst toward the formic acid oxidation is much enhanced over the Pd nanoparticles. As seen in Fig. 4B, the oxidation current on the Pd/Ni decays by ca. 56.3% after ca. 30 min polarization, whereas the oxidation current on the Pd catalyst decays by ca. 96.5%. Two reasons might account for the improved catalytic activity and durability of the Pd/Ni for formic acid oxidation. At first, the variation of the electronic structure in the CUS atoms leads to an enhancement in CO-tolerance, verified by CO stripping. Secondly, the dissolution of the Ni species within the Pd/Ni nanocomposites, as confirmed by ICP-AES, may prevent the Pd atoms from corrosion since the standard potential of the PdCl$_4^{2-}$/Pd (0.591 V, vs. SHE) is higher than that of the Ni^{2+}/Ni (-0.257 V, vs. SHE)[15]. In reproducible measurements, 100 mL of the electrolyte was collected and evaporated to obtain 10 mL of the solution. The concentrations of Pd^{2+} ions in the electrolyte are 0.251 and 0.426 mg·L^{-1} after being polarized for 900 and 1800 s for the Pd/GC, respectively. For a comparison, the concentrations of Pd^{2+} ions for the Pd/Ni GC are 0.152 and 0.201 mg·L^{-1}, and the Ni^{2+} ions were 0.307 and 0.427 mg·L^{-1}. Therefore, the Pd/Ni ratio on the GC after being test for 30 min is 4.1:1, estimated from the ICP-AES results.

4　Conlusions
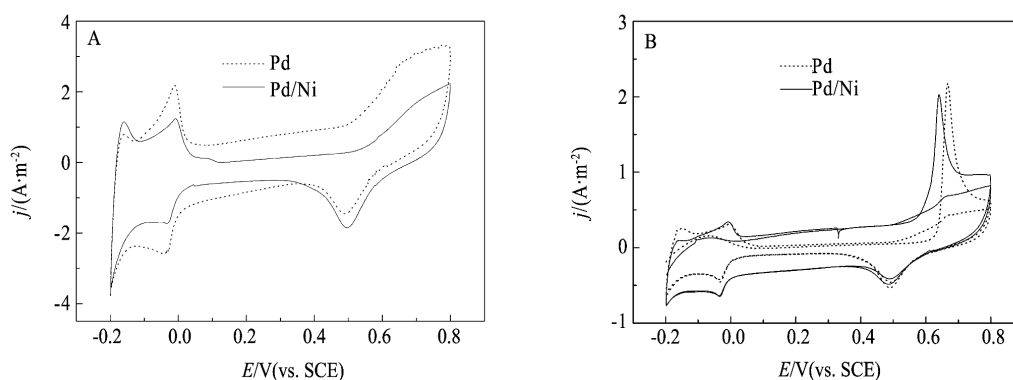
　　In summary, the Pd/Ni heterostructured catalyst

Fig. 3 CVs and CO-stripping voltammograms at a scan rate of 20 mV·s^{-1} in 0.5 mol·L^{-1} H$_2$SO$_4$. The current densities are normalized to ECSAs$_H$ in Fig. 3A and to ECSAs$_{CO}$ in Fig. 3B.
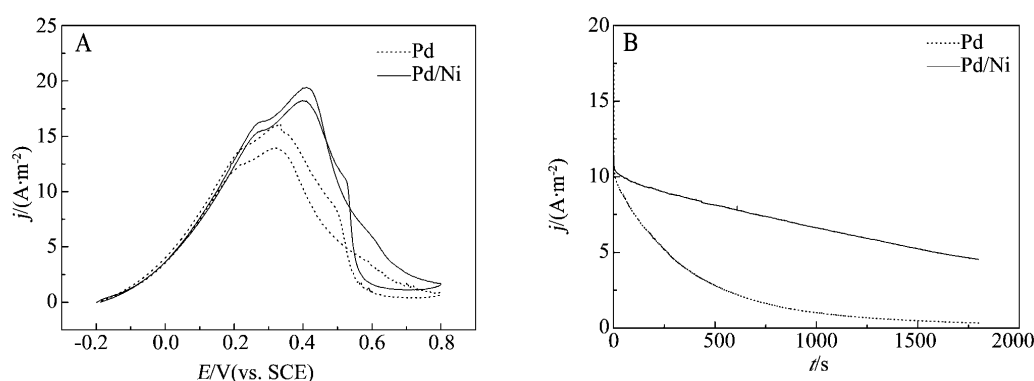
Fig. 4 CVs at a scan rate of 50 mV·s⁻¹ and CA curves at a given potential of 0.16 V vs. SCE for formic acid oxidation on the Pd and Pd/Ni catalysts in 0.5 mol·L⁻¹ HCOOH + 0.5 mol·L⁻¹ H₂SO₄. The current densities are normalized to the ECSAs_CO of the catalysts.

was successfully synthesized via a two-step reduction procedure. The electrocatalytic activity of formic acid oxidation on the heterostructured Pd/Ni is higher than that on pure Pd nanoparticles, and the durability of the Pd/Ni catalyst is greatly enhanced. The change in electronic structure of the surface CUS Pd atoms and the possible dissolution of the Ni species from the Pd/Ni heterostructure may account for such an improved catalytic activity and durability for the oxidation of formic acid.

Acknowledgements

References:

[1] Wang J Y, Zhang H X, Jiang K, et al. From HCOOH to CO at Pd electrodes: A surface-enhanced infrared spectroscopy study[J]. Journal of the American Chemical Society, 2011, 133(38): 14876-14879.

[2] Zhang H X, Wang S H, Jiang K, et al. In situ spectroscopic investigation of CO accumulation and poisoning on Pd black surfaces in concentrated HCOOH[J]. Journal of Power Sources, 2012, 199(1): 165-169.

[3] Yu X W, Pickup P G. Mechanistic study of the deactivation of carbon supported Pd during formic acid oxidation [J]. Electrochmistry Communications, 2009, 11 (10): 2012-2014.

[4] Ren M J, Kang Y Y, He W, et al. Origin of performance degradation of palladium-based direct formic acid fuel cells[J]. Applied Catalysis B: Environmental, 2011, 104 (1/2): 49-53.

[5] Wang X M, Xia Y Y. Electrocatalytic performance of Pd-Co-C catalyst for formic acid oxidation[J]. Electrochemistry Communications, 2008, 10(10): 1644-1646.

[6] Hann J L, Stafford K M, Morgan R D, et al. Performance of the direct formic acid fuel cell with electrochemically modified palladium-antimony anode catalyst[J]. Electrochimica Acta, 2010, 55(7): 2477-2481.

[7] Hammer B, Nørskov J K. Theoretical surface science and catalysis-calculations and concepts [J]. Advances in Catalysis, 2000, 45: 71-129.

[8] Ruban A, Hammer B, Stoltze P, et al. Surface electronic structure and reactivity of transition and noble metals[J]. Journal of Molecular Catalysis A: Chemical, 1997, 115 (3): 421-429.

[9] Bligaard T, Nørskov J K. Ligand effects in heterogeneous catalysis and electrochemistry[J]. Electrochimica Acta, 2007, 52(18): 5512-5516.

[10] Strasser P, Koh S, Anniyev T, et al. Lattice-strain control of the activity in dealloyedcore-shell fuel cell catalysts[J]. Nature Chemistry, 2010, 2(6): 454-460.

[11] Wang D S, Li Y D. Bimetallic nanocrystals: Liquid-phase synthesis and catalytic applications[J] Advanced Materials, 2011, 23(9): 1044-1060.

[12] Zhang S, Shao Y Y, Yin G P, et al. Electrostatic self-assembly of a Pt-around-Au nanocomposite with high activity towards formic acid oxidation[J]. Angewandte Chemie International Edition, 2010, 49(12): 2211-2214.

[13] Li R S, Wei Z, Huang T, et al. Ultrasonic-assisted synthesis of Pd-nialloycatalysts supported on multi-walled carbon nanotubes for formic acid electrooxidation [J]. Electrochimica Acta, 2011, 56(19): 6860-6865.

[14] Kibler L A, El-Aziz A M, Hoyer R, et al. Tuning reaction rates by lateral strain in a palladium monolayer[J].

Angewandte Chemie International Edition, 2005, 44 (14): 2080-2084.

[15] Oezaslan M, Heggen M, Strasser P. Size-dependent morphology of dealloyed bimetallic catalysts: Linking the nano to the macro scal[J]. Journal of the American Chemical Society, 2012, 134(1): 514-524.

Pd/Ni 异结构纳米催化剂的制备及其对甲酸氧化的电催化

任明军[1,2], 邹亮亮[1,2], 陈 举[1], 袁 婷[1], 黄庆红[1],
张海峰[1], 杨 辉[1*], 封松林[1]

(1. 中国科学院上海高等研究院, 上海 201210; 2. 中国科学院研究生院, 北京 100039)

摘要: 通过两步还原法制备了 Pd/Ni 双金属催化剂. 由于金属 Pd 原子在先行还原的 Ni 纳米粒子表面的外延生长以及其在 Ni 表面和 Pd 表面生长表现出的吉布斯自由能差异, 最终导致了异结构 Pd/Ni 纳米粒子的形成. 高分辨电子透射显微镜结果证实了异结构的存在, 然而 X 射线衍射测量表明 Pd/Ni 纳米粒子具有类似于 Pd 的面心立方结构. 制备的 Pd/Ni 纳米粒子与同等条件下合成的 Pd 纳米粒子相比, 对甲酸氧化呈现了更高的电催化活性, 而且电催化稳定性也要明显优于纯 Pd 纳米粒子, 证明了 Pd/Ni 双金属催化剂是可选的直接甲酸燃料电池阳极催化剂. 双金属催化剂对甲酸氧化电催化活性和稳定性增强可能是 Ni 原子的修饰改变了 Pd 粒子表面配位不饱和原子的电子结构所致.

关键词: 甲酸氧化; 电催化; Pd/Ni 双金属; 稳定性